Article

Enantioselective, Chirally Templated Sol–Gel Thin Films

Sharon Fireman-Shoresh, Inna Popov, David Avnir, and Sharon Marx

J. Am. Chem. Soc., **2005**, 127 (8), 2650-2655• DOI: 10.1021/ja0454384 • Publication Date (Web): 04 February 2005

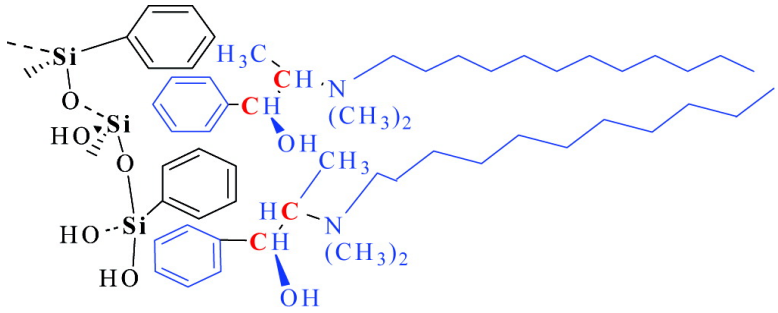

More About This Article

Additional resources and features associated with this article are available within the HTML version:

- Supporting Information
- Links to the 6 articles that cite this article, as of the time of this article download
- Access to high resolution figures
- Links to articles and content related to this article
- Copyright permission to reproduce figures and/or text from this article

View the Full Text HTML

J|A|C|S
ARTICLES
Published on Web 02/04/2005

Enantioselective, Chirally Templated Sol−Gel Thin Films

Sharon Fireman-Shoresh,[†] Inna Popov,[‡] David Avnir,[†] and Sharon Marx*[,§]

Contribution from the Institute of Chemistry and The Unit for Nanocharacterization, Faculty of Science, The Hebrew University of Jerusalem, Jerusalem 91904, Israel, and Department of Physical Chemistry, Israel Institute for Biological Research, Ness-Ziona 74100, Israel

Received July 29, 2004; E-mail: marx@intersun.iibr.gov.il

Abstract: Enantioselective surfactant-templated thin films were fabricated through the sol−gel (SG) process. The enantioselectivity is general in the sense that it discriminates between pairs of enantiomers not used for the imprinting process. The chiral cationic surfactant (−)-*N*-dodecyl-*N*-methylephedrinium bromide (**1**) was used as the surfactant template, and after its extraction chiral domains were created. The chiral discriminative feature of these films was examined by challenging with pure enantiomer solutions for rebinding. Selective adsorption was shown using (*R*)- and (*S*)-propranolol, (*R*)-**2** and (*S*)-**2**, respectively, and (*R*)- and (*S*)-2,2,2-trifluoro-1-(9-anthryl)ethanol, (*R*)-**3** and (*S*)-**3**, respectively, as the chiral probes. The selective adsorption was measured by fluorescence analysis, and the chiral selectivity factors were found to be 1.6 for **2** and 2.25 for **3**. In both cases, (*R*)-enantiomer was adsorbed preferably. The resulting material was characterized by transmission electron microscopy, by diffraction, and by surface area measurements, and was found to be semicrystalline with short-range ordered domains (50 Å) of hexagonal symmetry.

1. Introduction

Recently, we reported the successful imprinting of sol−gel thin films with a variety of molecules,[1,2] including chiral ones. Thus, films that were imprinted with a specific enantiomer showed clear preference to its re-adsorption, as compared to the opposite enantiomer. Here, we move an important step forward and describe the preparation of thin films which are generally enantioselective, where the chirally imprinted cavities can discriminate between enantiomers of molecules not used in the imprinting process, and completely different from the imprinting one. Chirally templated thin films are important for biomedical studies, for chiral catalysis, and for evaluating enantiomeric excess. The approach we use follows the preparation of porous (derivatized) silica matrices by templating with high concentrations of a surfactant, which has been a major direction in recent materials science. Interest in these materials stems from the many demonstrated useful applications, including shape selective catalysis, molecular sieving, chemical sensing and selective adsorption.[3−13] Sol−gel methodologies emerged as the preferred route of synthesis of these materials because they entail mild reaction conditions and offer a wide selection of metal alkoxide monomers, with which one can tailor chemical functionalities to the final porous material. The resulting templated sol−gel matrix can be obtained in various forms: monoliths, ground powders, or thin films. The latter, the topic of this report, have been fabricated by dip- or spin-coating[14−16] and offer advantages, which originate from the submicrometer thickness, including fast diffusion and transport needed for sensing.

Successful attempts to template chiral cavities within silica were reported, beginning with Curti et al. in 1952,[17] who obtained 30% enrichment of the templating enantiomer, continuing, for instance, in the studies of Che et al.,[18,19] Jung et al.,[20−23] Katz et al.,[24] Kunitake et al.,[25] Markowitz et al.,[26] and

[†] Institute of Chemistry, The Hebrew University of Jerusalem.
[‡] The Unit for Nanocharacterization, The Hebrew University of Jerusalem.
[§] Israel Institute for Biological Research.

(1) Fireman-Shoresh, S.; Avnir, D.; Marx, S. *Chem. Mater* **2003**, *15*, 3607−3613.
(2) Marx, S.; Zaltsman, A.; Turyan, I.; Mandler, D. *Anal. Chem* **2004**, *76*, 120−126.
(3) Brinker, C. J.; Lu, Y.; Sellinger, A.; Fan, H. *Adv. Mater* **1999**, *11*, 579−585.
(4) Lu, Y.; Cao, G.; Kale, R. P.; Prabakar, S.; Lopez, G. P.; Brinker, C. J. *Chem. Mater*. **1999**, *11*, 1223−1229.
(5) Lyu, Y.-Y.; Yi, S. H.; Shon, J. K.; Chang, S.; Pu, L. S.; Lee, S.-Y.; Eui, J.; Char, K.; Stucky, G. D.; Kim, J. M. *J. Am. Chem. Soc* **2004**, *126*, 2310−2311.
(6) Raman, N. K.; Anderson, M. T.; Brinker, C. J. *Chem. Mater*. **1996**, *8*, 1682−1701.
(7) Wang, J.; Zhang, J.; Asoo, B. Y.; Stucky, G. D. *J. Am. Chem. Soc.* **2003**, *125*, 13966−13967.
(8) Antonietti, M. *Curr. Opin. Colloid Interface Sci.* **2001**, *6*, 244−248.
(9) Tolbert, S. H.; Landry, C. C.; Stucky, G. D.; Chmelka, B. F.; Norby, P.; Hanson, J. C.; Monnier, A. *Chem. Mater*. **2001**, *13*, 2247−2256.
(10) Sierra, L.; Lopez, B.; Gil, H.; Guth, J.-L. *Adv. Mater*. **1999**, *11*, 307−311.
(11) Linssen, T.; Cassiers, K.; Cool, P.; Vansant, E. F. *Adv. Colloid Interface Sci.* **2003**, *103*, 121−147.
(12) Inagaki, S.; Guan, S.; Fukushima, Y.; Ohsuna, T.; Terasaki, O. *J. Am. Chem. Soc.* **1999**, *121*, 9611−9614.
(13) Burleigh, M. C.; Markowitz, M. A.; Spector, M. S.; Gaber, B. P. *Langmuir* **2001**, *17*, 7923−7928.
(14) Honma, I.; Zhou, H. S.; Kundu, D.; Endo, A. *Adv. Mater*. **2000**, *12*, 1532−1533.
(15) Hua, Z.-L.; Shi, J.-L.; Wang, L.; Zhang, W.-H. *J. Non-Cryst. Solids* **2001**, *292*, 177−183.
(16) Pavzner, S.; Regev, O.; Yerushalmi-Rozen, R. *Curr. Opin. Colloid Interface Sci.* **2000**, *4*, 420−427.
(17) Curti, R.; Colombo, U. *J. Am. Chem. Soc.* **1952**, *74*, 3961.
(18) Che, S.; Garcia-Bennett, A. E.; Yokoi, T.; Sakamoto, K.; Kunieda, H.; Terasaki, O.; Tatsumi, T. *Nat. Mater.* **2003**, *2*, 801−805.
(19) Che, S.; Liu, Z.; Ohsuna, T.; Sakamoto, K.; Terasaki, O.; Tatsumi, T. *Nature* **2004**, *429*, 281−284.
(20) Jung, J. H.; Ono, Y.; Hanabusa, K.; Shinkai, S. *J. Am. Chem. Soc.* **2000**, *122*, 5008−5009.

10.1021/ja0454384 CCC: $30.25

Seddon et al.,[27] but, as far as we can tell, although recognized as an important application, oxide thin-film general enantioselectivity toward foreign, nonanalogous pairs of enantiomers has not been reported and is the main novelty of this report.

The surfactant of choice for our studies has been the cationic (1*R*,2*S*)-(−)-*N*-dodecyl-*N*-methylephedrinium bromide (DMB), **1**, which possesses two chiral centers. The surfactant was entrapped at supercritical micelle concentrations (cmc) within a 20%-phenylated silica sol−gel film (thickness of 265.6 ± 16.5 nm) that was then extracted from the film with alcohol. Evaluation of the enantioselective character of the resulting chirally imprinted film was performed with the antihypertnsive drug (*S*)-propranolol, (*S*)-**2**, and its enantiomer (*R*)-**2**, and with the chiral NMR shift reagent 2,2,2-trifluoro-1-(9-anthryl)ethanol ((*S*)-**3** and (*R*)-**3**).[28]

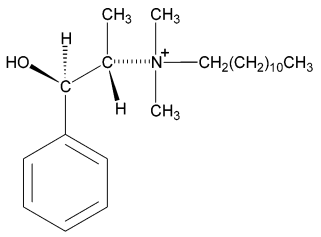

1

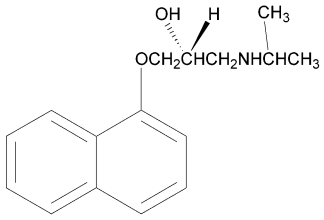

(R)-**2**

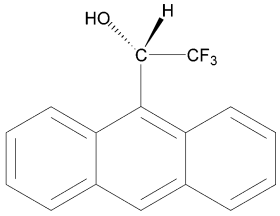

(S)-**3**

2. Experimental Details

Entrapment of the Chiral Surfactant DMB within the Sol−Gel Film (DMB@SG). The procedure of the film preparation is a modification of the procedure of Honma et al.:[14] 1.1 mL (7.40 mmol) of TMOS, 0.34 mL (1.87 mmol) of PTMOS, and 4.3 mL of 1-propanol were mixed. Next, 0.8 mL of 1 M HCl and 0.5 mL of H_2O were mixed separately and were than added dropwise to the silanes mixture. After 1 h of stirring at room temperature (RT), 2.2 mL of 1-butanol was added, and the stirring was continued for further 30 min. DMB (50 mg) was dissolved in 1.1 mL of H_2O (0.11 M). The solution was added to the above solution, and the combined mixture was stirred for additional 2 h at RT. The solution molar ratio is Si:H_2O:1-propanol:2-butanol:HCl = 1:9.5:6.2:2.6:2.4, and the final surfactant concentration is 0.011 M. Glass plates (BDH, 12 mm diameter) or silicon chips (1 × 2 cm, used to determine the thickness of the film) were spin-coated (Laurell, WS400A-lite) by placing 30 μL of the solution on the plate and spinning for 20 s at 4000 rpm. All plates were allowed to polymerize and dry overnight in a covered Petri dish.

Entrapment of DMB in Bulk Sol−Gel Matrices. The excess of the solution that was used for the film casting was left to gel in a coated vial at RT for 1 week. Final drying was achieved after 3 days of heating at 50 °C. The dried monolith, bulk DMB@SG, was ground and used for several characterization measurements, as described below.

Surfactant Removal. Surfactant removal was achieved either by solvent extraction (in the case of glass plated films and for the monoliths) or by calcinations (in the case of silicon chip coatings). Solvent extraction was preformed by placing the glass plates or the ground monolith in a Soxhlet extractor with refluxing methanol for 24 h. Calcination was carried out at 400 °C for 1 h in air.

Enantioselectivity Binding Experiments. The extracted films were incubated in 2.0 mL of 1.0 μM solution of the selected enantiomer in basic phosphate buffer (BPB) for **2** or acidic phosphate buffer (APB) for **3** for 24 h at 25 °C. The plates were then rinsed with the same buffer solution followed by extraction of the bound species into 3.0 mL of ethanol (2 h at 25 °C). The concentrations of the extracted enantiomers were determined by fluorescence measurement (PTI-Photon Technology International fluorimeter) at the suitable spectral regions (λ_{ex} = 288 and 366; λ_{em} = 335 and 431 nm for **2** and **3**, respectively) using calibration curves. Each experiment was repeated for four different plates. Similar procedures (with variations detailed below) were employed for the nonextracted and calcined films.

Material Characterization. Surface Area Measurements. N_2 gas adsorption analysis was performed on the extracted monoliths using a Micromeritics ASAP 2000. The surface area was calculated using the BET equation.

Transmission Electron Microscopy and Diffraction Measurements. TEM and diffraction analyses were performed on a Philips CM 12 microscope operating at 100 kV and also on an Analytical transmission electron microscope Tecnai F20 G^2 (FEI). Samples were prepared by deposition of ethanolic dispersions of the material on Formvar or Carbon 300 mesh copper grid. The dispersions were air-dried for 1 min, and the extra solution was blotted off. The dispersions were prepared either by scratching the thin films coated on glass substrates to ethanol or by dispersing the monolith powder in ethanol.

X-ray Diffraction Measurements. XRD analysis was performed via a Bruker AXS diffractometer D8 Advance. The source was Cu Kα radiation (wavelength 1.54056 Å).

3. Results and Preliminary Discussion

A. The Enantioselectivity of the DMB-Imprinted Films toward Propranolol (2). Selective re-binding experiments of the enantiomers of **2** to the methanol-extracted DMB@SG films, **SG-imp-1**, were carried out as described above. Three reference films were investigated for their adsorption of **2**: the as-synthesized, unextracted DMB@SG (**1**@SG) film (**SG-ref-A**); the calcined DMB@SG (**SG-ref-B**); and the methanol extracted achiral-CTAB templated film (**SG-ref-C**). Figure 1 shows the binding of (*R*)-**2** and (*S*)-**2** to all films. As seen in Figure 1, **SG-imp-1** films showed a 1.6 preferential readsorption factor of (*R*)-**2** over the (*S*)-**2** enantiomer (0.624 ± 0.024 nmol vs 0.393 ± 0.017 nmol, respectively).

As can be seen from Figure 1, the three reference films adsorbed remarkably less than **SG-imp-1**. The aim of testing unextracted DMB@SG reference films (**SG-ref-A**) was to find out whether there is a possibility that unextracted chiral surfactant molecules that may have remained in the matrix serve as the enantioselective sites. As seen in Figure 1, **SG-ref-A** films show no enantiomeric preference (0.063 ± 0.003 nmol adsorption of (*R*)-**2** vs 0.067 ± 0.003 nmol of (*S*)-**2**). In addition, the amount adsorbed on this film is about 10-fold smaller than the

(21) Jung, J. H.; Kobayashi, H.; Masuda, M.; Shimizu, T.; Shinkai, S. *J. Am. Chem. Soc.* **2001**, *123*, 8785−8789.
(22) Jung, J. H.; Ono, Y.; Shinkai, S. *Angew. Chem., Int. Ed.* **2000**, *39*, 1862−1865.
(23) Jung, J. H.; Ono, Y.; Shinkai, S. *Chem.-Eur. J.* **2000**, *6*, 4552−4557.
(24) Katz, A.; Davis, M. E. *Macromolecules* **1999**, *32*, 4113−4121.
(25) Kunitake, T.; Lee, S.-W. *Anal. Chim. Acta* **2004**, *504*, 1−6.
(26) Markowitz, M. A.; Kust, P. R.; Klaehn, J.; Deng, G.; Gaber, B. P. *Anal. Chim. Acta* **2001**, *435*, 177−185.
(27) Seddon, A. M.; Patel, H. M.; Burkett, S. L.; Mann, S. *Angew. Chem., Int. Ed.* **2002**, *41*, 2988−2991.
(28) Pirkle, W. H.; Sikkenga, D. L.; Pavlin, M. S. *J. Org. Chem.* **1977**, *42*, 384−387.

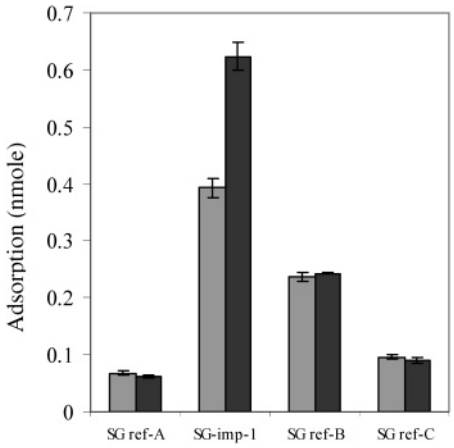

Figure 1. Fluorescent assay for (*S*)-**2** (gray bars) and (*R*)-**2** (black bars) adsorption to unextracted DMB@SG and to the reference thin films (λ_{ex} = 288 nm, λ_{em} = 335 nm), n = 4.

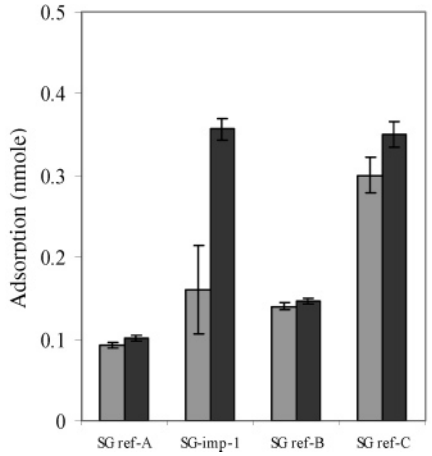

Figure 2. Fluorescent assay for (*S*)-**3** (gray bars) and (*R*)-**3** (black bars) adsorption to DMB@SG and to the reference thin films (λ_{ex} = 366 nm, λ_{em} = 431 nm), n = 4.

that on the extracted **SG-imp-1** film (when comparing the adsorption of (*R*)-**2**). We propose that the adsorption on **SG-ref-A** is on its outer surface and within its limited accessible porosity. Indeed, comparative surface area analysis on the related unextracted and extracted DMB@SG bulk materials provides supporting evidence, in that the surface areas differ significantly: 13.5 ± 0.1 and 375.5 ± 6.1 m^2/g, respectively. The adsorption results on **SG-ref-A** indicate that the chiral surfactant by itself does not give rise to enantioselection. Thus, even if some residual DMB is left after extraction, the observed enantiomeric discrimination is not due to its traces in the matrix, but rather to the chirally templated cavities. Why does the chiral cavity work better than a chiral templating molecule that was used to make it? Apparently, the cavity offers more contact sites that surround much of the **2** molecule, as compared to fewer sites, perhaps only one, in contact between **2** and DMB.

SG-ref-B was prepared to test whether the calcination mode of removal of the surfactant (common in the preparation of MCM materials[31,32]) preserves the fine, recognizing structure of the cavity. As seen in Figure 1, there is no apparent enantioselectivity: 0.243 ± 0.002 nmol of (*R*)-**2** vs 0.237 ± 0.007 nmol of (*S*)-**2**. Calcination is also known to close off sol−gel-generated pores,[33−35] which is reflected in the lower adsorption levels, seen in Figure 1. Thus, we believe that chiral induction in the thin film by templating creates in our case (cf., ref 19) a very delicate enantio-discriminative structure that can easily be destroyed by the calcination process, which causes a collapse of the fine arrangement of molecular moieties within the cage.

The third reference film, **SG-ref-C**, which was templated with the achiral surfactant CTAB followed by its extraction, was prepared to make sure that the observed recognition is due to the chiral nature of the templating DMB. Indeed (Figure 1), the adsorption values, 0.091 ± 0.004 nmol of (*R*)-**2** and 0.096 ± 0.004 nmol of (*S*)-**2**), both are remarkably lower than the binding observed for **SG-imp-1**, confirming the authenticity of the chiral induction by DMB.

B. The Enantioselectivity of the DMB-Imprinted Films toward 1,1,1-Trifluoro(anthryl)ethanol (3). The previous case demonstrated that the templated cavity is capable of recognizing chirality of a molecule that is different from the templating molecule. Our next example strengthens this observation with an entirely different chiral molecule, **3**. The enantioselectivity of extracted **SG-imp-1** toward the enantiomers of **3** is shown in Figure 2, along with a similar set of reference measurements.

Thus, it is seen that **SG-imp-1** adsorbs 0.36 ± 0.01 nmol of (*R*)-**3** but only 0.16 ± 0.05 nmol of (*S*)-**3**; that is, the adsorption equilibrium discrimination ratio is even larger (by a factor of 2.25) than the ratio obtained for **2**. Such preference to (*R*)-**3** was not revealed by any of the reference films. **SG-ref-A**, the unextracted DMB@SG, again shows that the chirality of the DMB molecules is insufficient for the enantioselectivity (adsorption of 0.100 ± 0.004 nmol of (*R*)-**3** vs 0.093 ± 0.004 nmol of (*S*)-**3**) and that it is the chiral cage that is indeed needed for that type of recognition. **SG-ref-B**, the calcined DMB@SG, again shows that calcination causes a loss of enantioselectivity. The adsorption values (for (*R*)-**3** and (*S*)-**3**, 0.146 ± 0.003 and 0.140 ± 0.004 nmol, respectively) are somewhat lower as compared to those obtained for **2**, indicating the action of **SG-ref-B** as a general porous silica adsorbent. The better enantioselectivity of **SG-imp-1** toward **3** as compared to **2** can be understood by noticing that **SG-ref-C** (the extracted achiral CTAB@SG) shows significantly higher adsorption affinity toward **3** (0.350 ± 0.015 nmol of (*R*)-**3** as compared to 0.091 ± 0.004 nmol of (*R*)-**2**). Thus, the better enantioselectivity toward the enantiomers of **3** can be rationalized by the better interaction of that molecule with the phenyl-rich silica surface.

C. TEM and XRD Measurements. Beyond the phenomenological aspect of achieving chiral recognition, we were also interested in getting some insight into the structure of the recognizing films and performed TEM observations and XRD analyses for that purpose. Let us begin with the bottom-line and then fill-up the supporting evidence for the conclusion: The structure of the films is characterized by short-range ordered domains from a few angstroms up to ~50 Å in size, the

(29) Xiao, T. L.; Rozhkov, R. V.; Larock, R. C.; Armstrong, D. W. *Anal. Bioanal. Chem.* **2003**, *377*, 639−654.
(30) Kurata, K.; Shimoyama, T.; Dobashi, A. *J. Chromatogr., A* **2003**, *1012*, 47−56.
(31) Yang, P.; Zhao, D.; Margolese, D. I.; Chmelka, B. F.; Stucky, G. D. *Nature* **1998**, *396*, 152−155.
(32) Kleitz, F.; Schmidt, W.; Schüth, F. *Microporous Mesoporous Mater.* **2003**, *65*, 1−29.
(33) Dumas, R. L.; Tejedor-Tejedor, I.; Anderson, M. A. *J. Porous Mater.* **1998**, *5*, 95−101.
(34) Huang, W. L.; Liang, K. M.; Cui, S. H.; Gu, S. R. *J. Colloid. Interface Sci.* **2000**, *231*, 152−157.
(35) Klein, L. C.; Gallo, T. A. *J. Non-Cryst. Solids* **1990**, *121*, 119−123.

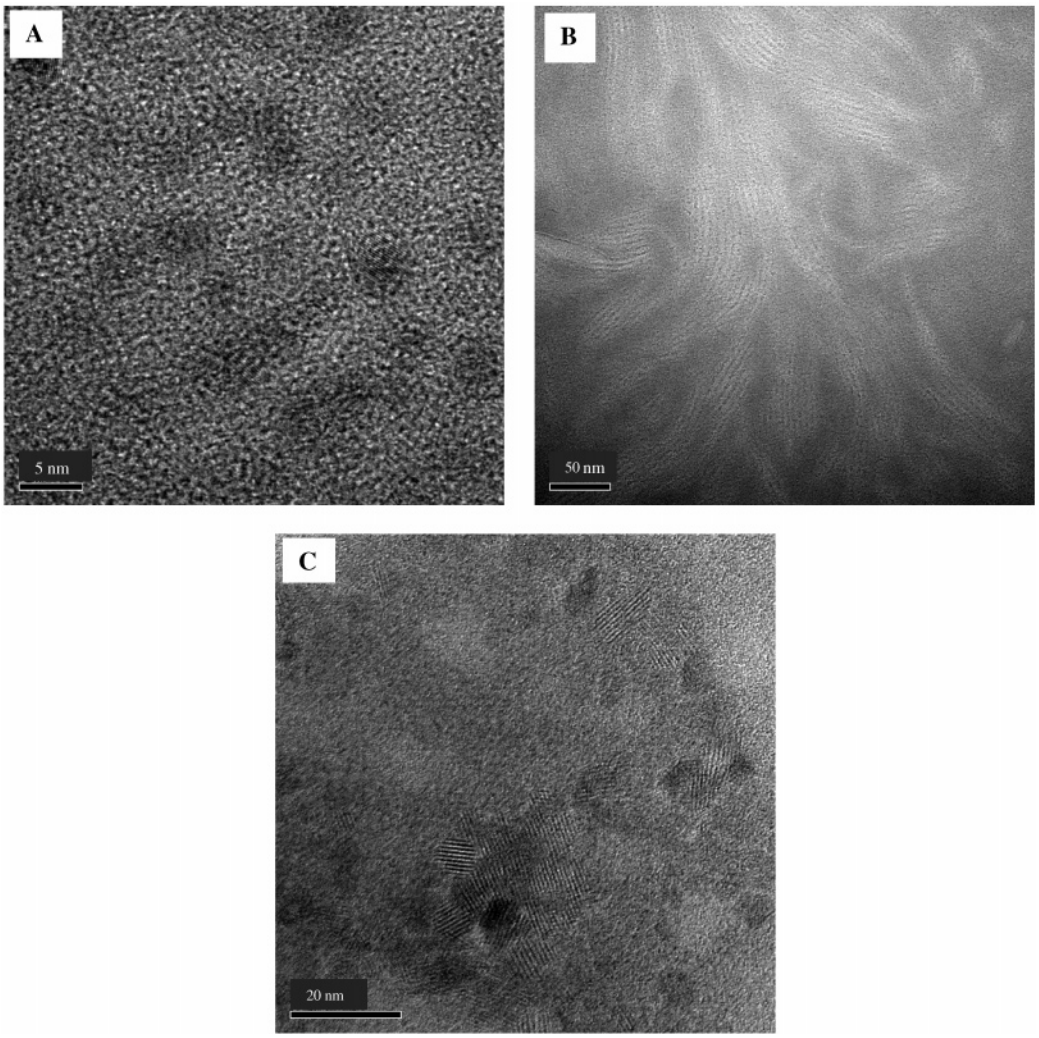

Figure 3. TEM images of DMB@SG thin film (A,B) before extraction and (C) after extraction.

symmetry of which is hexagonal trydimite, which is oriented randomly, with no long-range order. Some details follow.

TEM images of the sol−gel thin film before and after surfactant extraction (**SG-ref-A** and **SG-imp-1**) are shown in Figure 3.

The oriented domains and the semicrystalline nature of the material are clearly seen from Figure 3C with *d* spacings of 2.25 ± 0.52 and 4.19 ± 0.03 nm for the film before surfactant removal, and 2.39 ± 0.37 nm after removal. Because the oriented domains induce semicrystallinity, ring-type SADs (selected area diffraction patterns) could be obtained (Figure 4).

Radii analysis of the rings (using $d = \lambda L/r$, where λ is the wavelength of the electrons in the primary electron beam, L is the work distance of the microscope, and r is the distance between the diffraction rings) indicated that the material is packed in a hexagonal symmetry (the array of ratios of *d* values is summarized in Table 1). Comparing the absolute values of the *d* spacings as calculated from SADs to those for known hexagonal phases of silica,[36] we can conclude that the tested material is similar to known hexagonal trydimites (JSPDS cards 89-3141 and 89-3608).

(36) Gorelik, S. S.; Skakov, U. A.; Rastorgnev, L. N. *Analysis of X-ray and Electron Diffraction*, 3rd ed.; Mises University: Moscow, 1994.

Under the cautionary comment that bulk materials do not necessarily reflect thin film behavior, we shall now mention supportive XRD data obtained for the extracted DMB@SG monolith (Figure 5).

This pattern characterized a material with short-range order in which the possible *d* spacings are around three most probable values of 4, 20, and 44 Å.

It is seen that the spectrum contains only three broad peaks at low scattering angles and no sharp peaks at all. This means that the material is disordered on the long-range scale, but does have a short-range ordering. This short-range order is characterized by several spacings around three most probable values of 4, 20, and 44 Å, defined by the positions of the broad peaks maxima. The most probable minimum interatomic distance is therefore around 4 Å, while the maximal ordered domain size is, most probably, around 44 Å. Note that the two longer specific distances of 20 and 44 Å are multiples of 4, which allows one to interpret the structural units of the tested material as various combinations of 4 Å-size elemental "cells". We recall that in most papers dealing with MCM-derived materials the XRD shows a sharp peak at $2\theta = 2°$ and the d_{100} is ∼44 Å.[37−39]

4. Further Discussion and Conclusions

In this work, we synthesized chirally templated sol−gel thin films, capable of enantioselective adsorption of molecules

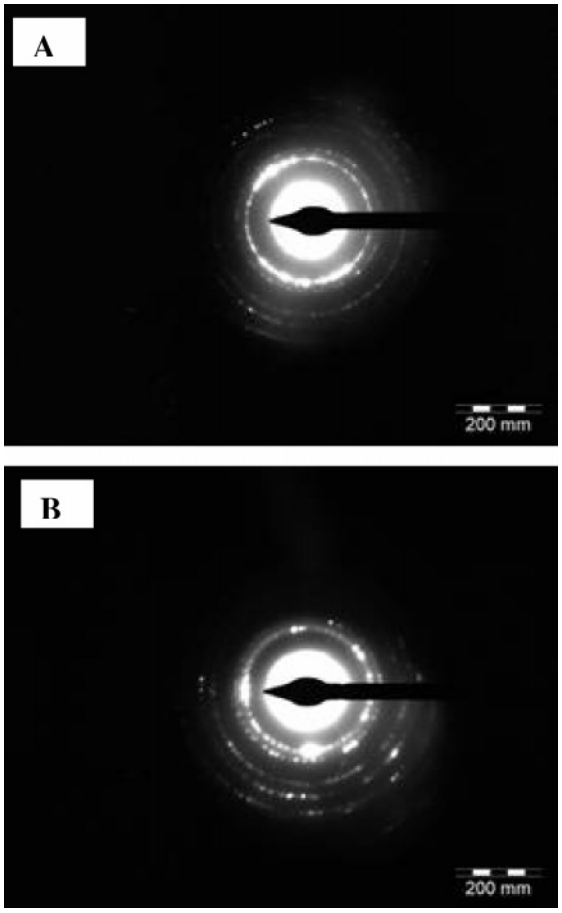

Figure 4. SAD patterns of DMB@SG thin film (A) before extraction and (B) after extraction.

Table 1. *d*-Spacing Values Recalculated from the SADs

d (Å)	$d_{h_ik_il_i}{}^2$ (Å^2)	$d_{h_ik_il_i}{}^2/d_{h_1k_1l_1}{}^2$
3.97	15.7609	1
2.33	5.4289	2.90
1.99	3.9601	3.98
1.45	2.1025	7.50

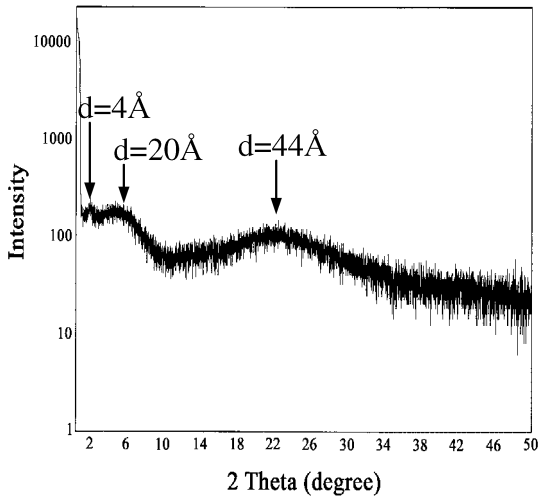

Figure 5. Powder X-ray diffraction pattern of DMB@SG monolith after surfactant extraction.

unrelated to the imprinting one. The design step is very important and crucial in the molecular imprinting process. In this step, the monomers are chosen due to their functional group to improve the imprinting process of the template molecule and facilitate its rebinding. Because the aim of this work was not to create a molecular recognition site with the shape of the template molecule but to induce general chirality by supramolecular arrays, the right combination of hydrophilicity/hydrophobicity (TMOS/PTMOS monomers) was needed to allow recognition that is based on chirality, and not on specific shapes. The phenyl group can interact through $\pi-\pi$ bonding with the aromatic ring of **1** at the templating stage, and also can promote

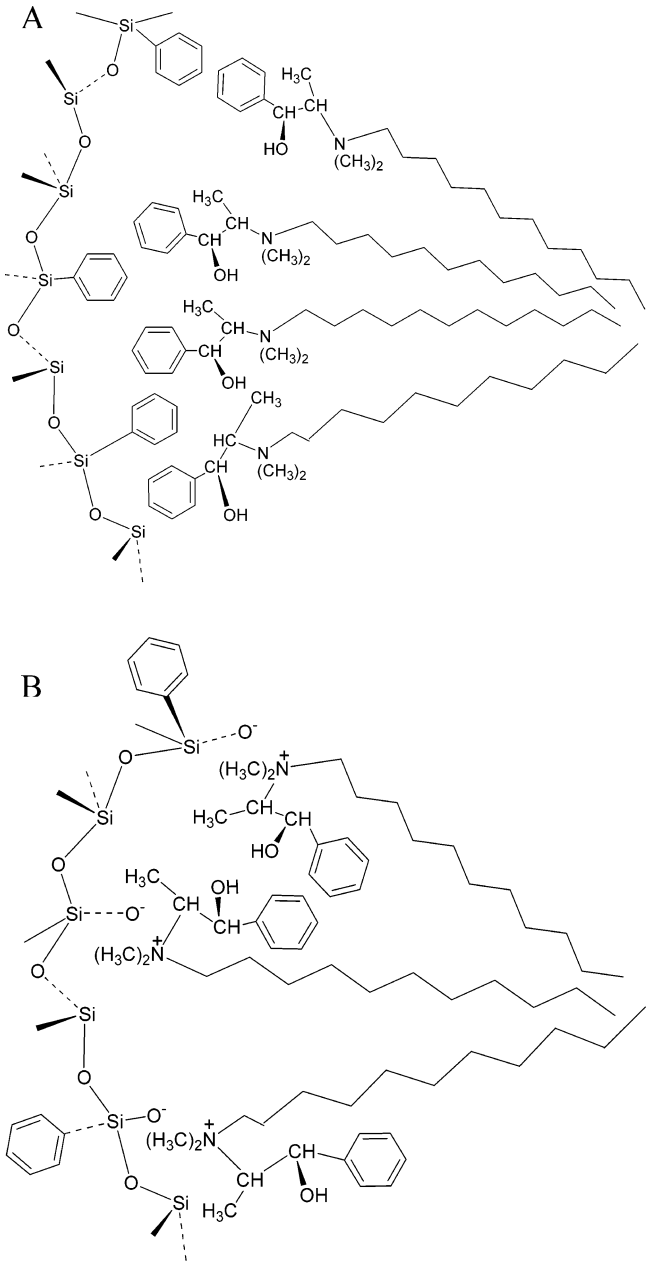

Figure 6. Schematic illustration of two types of interactions between the surfactant chiral headgroup and the sol−gel matrix. (A) The surfactant interacts through a $\pi-\pi$ interaction. (B) Electrostatic attraction between the negative charged silica and the surfactant cationic quaternary ammonium.

(37) Burleigh, M. C.; Markowitz, M. A.; Spector, M. S.; Gaber, B. P. *J. Phys. Chem. B* **2001**, *105*, 9935−9942.
(38) Ciesla, U.; Schüth, F. *Microporous Mesoporous Mater.* **1999**, *27*, 131−149.
(39) Huo, Q.; Margolese, D. I.; Stucky, G. D. *Chem. Mater.* **1996**, *8*, 1147−1160.

$\pi-\pi$ interaction with the naphthyl group of **2** and the anthracene residue of **3** during the recognition stage. Likewise are used the hydrophilic Si−OH and the hydrophobic Si−O−Si moieties.

From XRD and TEM results, it is clear that the resulted structure contains two types of domains: ordered and disordered, where the ordered domains are characterized by hexagonal trydimite symmetry in local arrangement, and which are embedded in the disordered bulk. Where then does the enantioselective discrimination take place? There are two possible options (Figure 6): A basic assumption, supported by the general knowledge accumulated for surfactant templating, is that the long hydrophobic chains point away from the silica backbone. The surfactant can interact with the formed matrix either through $\pi-\pi$ interactions (Figure 6a) or through electrostatic attraction in a folded manner as shown in Figure 6b. This surfactant orientation is supported by the *d*-spacing values that were obtained from the TEM measurements. In the first suggested orientation (Figure 6a), the surfactant length is 2.4 nm, and in the latter orientation (Figure 6b) it is 1.85 nm.

The surfactants can aggregate in micelle-like or in hemimicelle structures, apparently leading to the measured values of ∼4 and ∼2 nm, respectively. In both cases, the chiral headgroup is close to the silica backbone, which again raises the question: Which domain is the chiral one? One assumption can be that the crystalline microstructures are chiral (we recall that Che et al. reported a proposed-twisted hexagonal packing[19]) and therefore the enantioselective adsorption occurs only in there. Another option is that the chiral surfactant aggregates induce their chirality in the amorphous areas of the silica SiO_2 in a manner which resembles imprinting with nonsurfactant molecules as we reported previously.[1] However, comparing the selective adsorption results in this paper to our previous reported results,[1] it can be seen that by templating with a surfactant, we achieved higher adsorption values (ca. 2−3 times fold) than in our last finding; that is, we have here a significantly higher chiral area. Thus, although we are not ready yet to propose a distinct answer to the question of the recognition site, we do propose that the enantioselective adsorption probably occurs in the two possible chiral domains, the ordered one and the disordered one.

Acknowledgment. We thank Mrs. Ruth Govrin from the TEM unit at the Silverman Institute for Biology, The Hebrew University of Jerusalem. Financial support from the Israel Ministry of Science, Culture, and Sports is gratefully acknowledged.

Supporting Information Available: Experimental data of the chemical used, determination of DMB cmc, and the procedure for entrapment of CTAB in sol gel. This material is available free of charge via the Internet at http://pubs.acs.org.

JA0454384